



Bioluminescent calcium mediated detection of nanosecond electroporation: Grasping the differences between 100 ns and 100 μ s pulses

Vitalij Novickij^{a,*}, Auksė Zinkevičienė^b, Eivina Radzevičiūtė^b, Julita Kulbacka^c,
Nina Rembiałkowska^c, Jurij Novickij^a, Irutė Girkontaitė^b

^a Faculty of Electronics, Vilnius Gediminas Technical University, Vilnius, Lithuania

^b State Research Institute Centre for Innovative Medicine, Department of Immunology, Vilnius, Lithuania

^c Department of Molecular and Cellular Biology, Faculty of Pharmacy, Wrocław Medical University, Wrocław, Poland

ARTICLE INFO

Keywords:

Calcium electroporation
Bioluminescence
Membrane permeabilization
Kinetic measurement
nsPEF

ABSTRACT

Electroporation is a phenomenon of transient or irreversible permeabilization of the cell membrane after pulsed electric field treatment. Fluorescent probes are frequently used to assess the extent of permeabilization, however, as an alternative, a D-luciferin oxidation-based method can be used. In this work, we have used sequences of a microsecond (1.3 kV/cm \times 100 μ s) and nanosecond (12.5 kV/cm \times 100 ns) pulses to trigger various levels of cell permeabilization and assessed the differences in the response using a conventional fluorescent probe (YO-PRO-1 (YP)) and D-luciferin oxidation methodology. The nanosecond pulses ($n = 5$ –100) have been delivered with 1 kHz repetition frequency, and the results were compared with 1 MHz protocols. Additionally, the effects of extracellular Ca^{2+} have been assessed. Various concentrations of CaCl_2 (2, 5, and 10 mM) have been used, and it was shown that the bioluminescence of the cells after electroporation depends on extracellular calcium concentration. It was shown that the changes in bioluminescence signal could be used as a marker of cell membrane permeabilization on par with YP assay when calcium is added and thus, effectively employed for analysis of electroporation phenomenon *in vitro* both for nanosecond and microsecond pulses.

1. Introduction

High intensity pulsed electric fields (PEF) can cause electropermeabilization of the cell membrane, also known as electroporation (EP), which is employed in gene and drug delivery, cancer treatment, food processing and biotechnology [1–6]. EP efficacy and type (reversible or irreversible) depend on PEF parameters [7,8]. As a result, the parametric analysis of EP and the subsequent biophysical effects is a major part of ongoing research and quick/easily reproducible methods to detect cell membrane permeabilization after PEF are required [9–11].

Application of PEF creates hydrophilic pores in the lipid bilayer and, during electroporation, initially non-permeant molecules (e.g., hydrophilic or large molecules) can cross the lipid bilayer to serve as an EP marker [9]. Fluorescence detection of the entry or leakage of ions or dyes is by far the most common method of detection and characterization of membrane electropermeabilization [10]. Propidium iodide (PI) and YO-PRO-1 (YP) can be highlighted as one of the most popular fluorescent probes used in this context [12–14]. When the membrane

integrity is compromised, the dyes enter the cell and bind to nucleic acids, resulting in a detectable fluorescence signal [10]. Nevertheless, the size of the dye affects the molecular entry, and thus the sensitivity of various dyes varies [10]. It is particularly important during weak electroporation or when ultrashort (nanosecond range) pulses are used. Taken that YP is a smaller dye molecule than PI [15], it is a better marker to detect the permeabilization of cell membrane caused by nanosecond pulsed electric fields (nsPEF) [16]. At the same time, YP is less sensitive for the determination of electroporation compared to the Ca^{2+} ions, which can be used as a marker when the cells are loaded with fluorophores like fura-2 [17,18]. Choosing the suitable detection method for various electroporation ranges is an important factor for accurate interpretation of the PEF triggered biophysical phenomena.

As an alternative to fluorescent probes, in our previous study, we have proposed a new *in vitro* electroporation detection model and method based on bioluminescence (i.e., D-luciferin oxidation) [19]. Mice myeloma cell line (Sp2/0) has been transfected with Luciferase-pcDNA3 plasmid, and it was shown that oxidation of D-luciferin

* Corresponding author at: Electronics Faculty, Naugarduko g. 41, LT-03227 Vilnius, Lithuania.

E-mail address: vitalij.novickij@vilniustech.lt (V. Novickij).

sodium salt can be successfully utilized to assay electroporation via the expression of the luciferase gene. The luminescence signal increases several-fold when the electroporation is triggered and scales with electroporation intensity, while the sensitivity of the methodology is on par with propidium electrotransfer. At the same time, the proposed methodology serves as a viability indicator too (only viable cells luminesce). Therefore, the capability to detect both the reversible and irreversible EP without any changes in the experimental scheme or methodology can be highlighted as the main advantage. Nevertheless, the exact mechanism of interaction between the cell permeabilization and oxidation of D-luciferin is still unknown. We speculated [19] that it is likely that the phenomenon is connected with a downstream effect of Ca^{2+} , which comes into electroporated cells since it is a universal second messenger which affects multiple intracellular cascades [20], and can result in increased metabolism and/or increased ATP consumption [21–23].

In this work, we try to address this hypothesis and thus performed a series of experiments using 100 ns (nsPEF) and 100 μs (μsPEF) pulses without and with extracellular calcium (0–10 mM). The resultant kinetics of the luminescence signal with and without calcium have been investigated and compared (sensitivity-wise to detect EP) with the conventional YP methodology. The results of this study provide experimental proof that bioluminescence can be effectively employed for kinetic analysis of electroporation phenomenon *in vitro*.

Lastly, the effects of high (MHz range) and low (kHz range) frequency pulsing have been covered in this work. Previously it was shown that manipulation of the delay between the nanosecond pulses can significantly alter the efficiency of electroporation [24–26]. It is possible to manipulate the PEF treatment outcome without altering the total energy of the burst [27]. The high-frequency EP phenomenon is believed to occur due to the accumulation of the cellular transmembrane voltage potential (TMP) when the relaxation time of the cell membrane is longer than the delay between the pulses. This study provides experimental proof that the delay between nanosecond pulses can be effectively used as an additional parameter to derive new protocols for nsPEF-based treatments.

2. Materials and methods

2.1. Pulsed power setup

The experimental setup consisted of 3 kV, 100 ns–1 ms square-wave high-voltage pulse generator (VGTU, Vilnius, Lithuania) [28] and a commercially available electroporation cuvette with a 1 mm gap between electrodes (Biorad, Hercules, USA). The voltage applied to the cuvette was 130 V and 1.25 kV, corresponding to a 1.3 and 12.5 kV/cm electric field, respectively. The pulses were delivered in bursts of 1–8 (1 Hz) for μsPEF protocol (1.3 kV/cm \times 100 μs) and in 5–100 pulse bursts (1 kHz/1 MHz) for the nsPEF protocol (12.5 kV/cm \times 100 ns).

2.2. Cells

Initially, the Sp2/0 myeloma cells were electro-transfected (1.2 kV/cm \times 100 μs \times 4) with Luciferase-pcDNA3 plasmid (Adgene plasmid #18964) linearized with Bgl II. For electroporation, the cells were counted, and for each sample 2×10^6 of cells were resuspended in HEPES buffer (10 mM, Sigma) containing 250 mM sucrose (POCH, Poland) and 1 mM MgCl_2 . For calcium electroporation CaCl_2 was added for the final concentration of 2, 5, and 10 mM depending on the protocol. The electroporation buffer without added calcium was used as a control and reference.

2.3. Fluorescence detection assay

Cell permeabilization was evaluated using YP (Sigma-Aldrich, Burlington, MA, USA) and flow cytometry. The cells (45 μl) were mixed with YP (5 μl) for the final YP concentration of 1 μM . The 45 μl samples were

placed between the electrodes and treated by PEF followed by 10 min incubation at room temperature. Afterward, the samples were analyzed by flow cytometry (10,000 cells) using Amnis FlowSight Imaging Flow Cytometer (Luminex Corporation, Texas, USA). YP fluorescence was evaluated using a bandpass filter of 530/30 nm. A shift of fluorescence spectra and the cells in the defined gate (which was defined based on the untreated control) have been interpreted as fluorescence positive (permeabilized), while the cells outside the gate have been interpreted as non-fluorescent (non-permeabilized), which is a standard procedure in electroporation studies.

2.4. Bioluminescence detection assay

After electroporation 40 μl of the cells were transferred into the white 96-well plates. D-Luciferin (Promega, USA) was added to the cells at a final concentration of 150 $\mu\text{g}/\text{ml}$. The luminescence of SP2/0 cells was evaluated using a Synergy 2 microplate reader and Gen5 software (BioTek, USA) for 30 min with a 1.5 min time step.

2.5. Statistical analysis

One-way analysis of variance (ANOVA; $p < 0.05$) was used to compare different treatments. Tukey HSD multiple comparison test for the evaluation of the difference was used when ANOVA indicated a statistically significant result ($p < 0.05$ was considered as statistically significant). The data was post-processed in OriginPro software (OriginLab, Northampton, MA, USA). All experiments were performed at least in three repetitions, and the treatment efficiency was expressed as mean \pm standard deviation.

3. Results

In order to evaluate the applicability of D-luciferin oxidation methodology for detection of electroporation *in vitro*, as a reference, the effects of three different calcium concentrations on cellular bioluminescent response were tested (2, 5 and 10 mM). The results are summarized in Fig. 1.

It can be seen that the bioluminescence signal does not change in time, and the differences versus control are statistically insignificant ($P > 0.05$). Based on the established reference signal level, the experiments with the application of μsPEF were performed. The cells were treated by 1.3 kV/cm \times 100 μs PEF and the number of pulses was varied. The

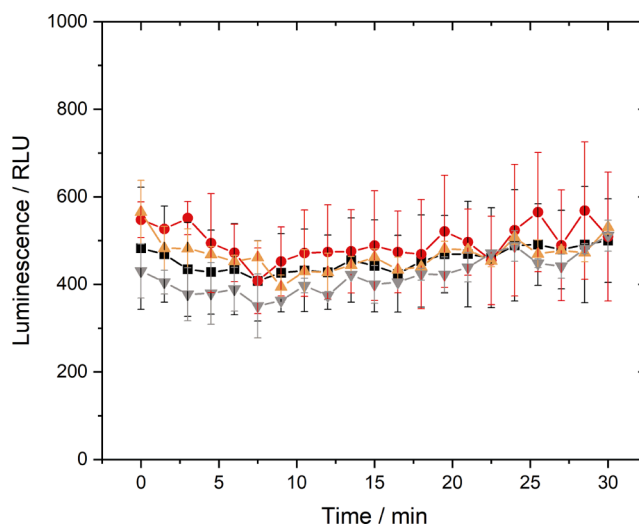


Fig. 1. Dependence of cell bioluminescence signal on calcium concentration in the buffer, where \blacksquare CTRL – buffer without added calcium; \bullet 2 mM CaCl_2 ; \blacktriangle 5 mM CaCl_2 ; \blacktriangledown 10 mM CaCl_2 .

results are summarized in Fig. 2.

As it can be seen in Fig. 2A, electroporation triggers a significant increase in the bioluminescence signal, which scales with the increase of the number of pulses at $t = 0-10$ min. The effects of 2 mM added calcium on the bioluminescence signal are shown in Fig. 2B. It's apparent that at $t = 0$ min, the signal is significantly higher than electroporation alone. An increase of the calcium concentration to 5 mM (Fig. 2C) did not result in significant changes of the peak RLU compared to the 2 mM (Fig. 2B). However, a dose-dependent response (pulse number-wise) was observed, affecting the kinetics of the signal. In the 0–5 mM calcium concentration range, the RLU signal increased with the treatment intensity – the $100 \mu\text{s} \times 8$ protocol featured the highest luminescence at $t = 0$ min. The drop of the signal below the control level (~ 500 RLU) was faster using $100 \mu\text{s} \times 8$ pulsing protocol. In the case of 10 mM CaCl_2 concentration, the same tendency of the response was also present. However, the peak value of the luminescence was significantly lower compared to 2 mM and 5 mM instances (Fig. 2D).

Next, the effects of nsPEF electroporation were studied in the same manner. The effects of $12.5 \text{ kV/cm} \times 100 \text{ ns}$ pulses were analyzed using 1 kHz and 1 MHz pulsing to trigger the TMP accumulation phenomenon, and the differences between the responses were evaluated. The results for the 1 kHz nsPEF protocols are shown in Fig. 3.

Fig. 3A shows that nsPEF electroporation in the medium without added Ca^{2+} does not trigger any changes of bioluminescence regardless of the number of pulses. It does not necessarily mean the lack of electroporation, however, it shows that the effects are beyond the detection limits of the methodology. When calcium is added to the buffer (Fig. 3B), the bursts of 25, 50, and 100 pulses trigger a detectable increase of the bioluminescence. The changes are observed after 25 pulses, and the higher the Ca^{2+} concentration, the faster the drop of RLU compared to

untreated control is detected.

Further, the effects of MHz nanosecond pulses were evaluated, and the results are summarized in Fig. 4.

Similar to kHz pulsing, the MHz pulsing did not trigger a detectable increase of the bioluminescence signal when no additional calcium was used (Fig. 4A). However, when 2 mM calcium was added, the electroporation was easily detectable already after 10 pulses (Fig. 4B). Further increase of the Ca^{2+} concentration to 5 mM has returned even a more profound response for the $100 \text{ ns} \times 10$ pulses sequence (Fig. 4C). It was not the case with 10 mM Ca experiment (Fig. 4D), where the signal level was significantly inhibited. A similar tendency was also detectable during μsPEF procedure (Fig. 2D).

Finally, the bioluminescent response of the cells (at $t = 0$ min) was compared with permeabilization data acquired using conventional YP fluorescent assay. The results for μsPEF electroporation are shown in Fig. 5.

As it can be seen, a dose dependent response was observed. With the increase in the number of pulses, the fraction of YP fluorescent cells is also increased. The RLU response follows the same pattern ($R = 0.929$), indicating a strong positive correlation between the assays. However, the situation changes with added calcium. All the protocols trigger an increase in luminescence. However, the assay cannot be used to determine permeabilization quantitatively anymore. The same analysis was performed for nsPEF, and the results are shown in Fig. 6.

It can be seen (Fig. 6A) that 1 kHz pulsing results in weak permeabilization even after 100 pulses (28.5%). The MHz pulsing improves the situation with more than 90% YP-positive cells at the same treatment conditions. A definitive dose-dependent response is observed again, which is an expected result. In terms of bioluminescence, the methodology without added calcium was not effective in detecting

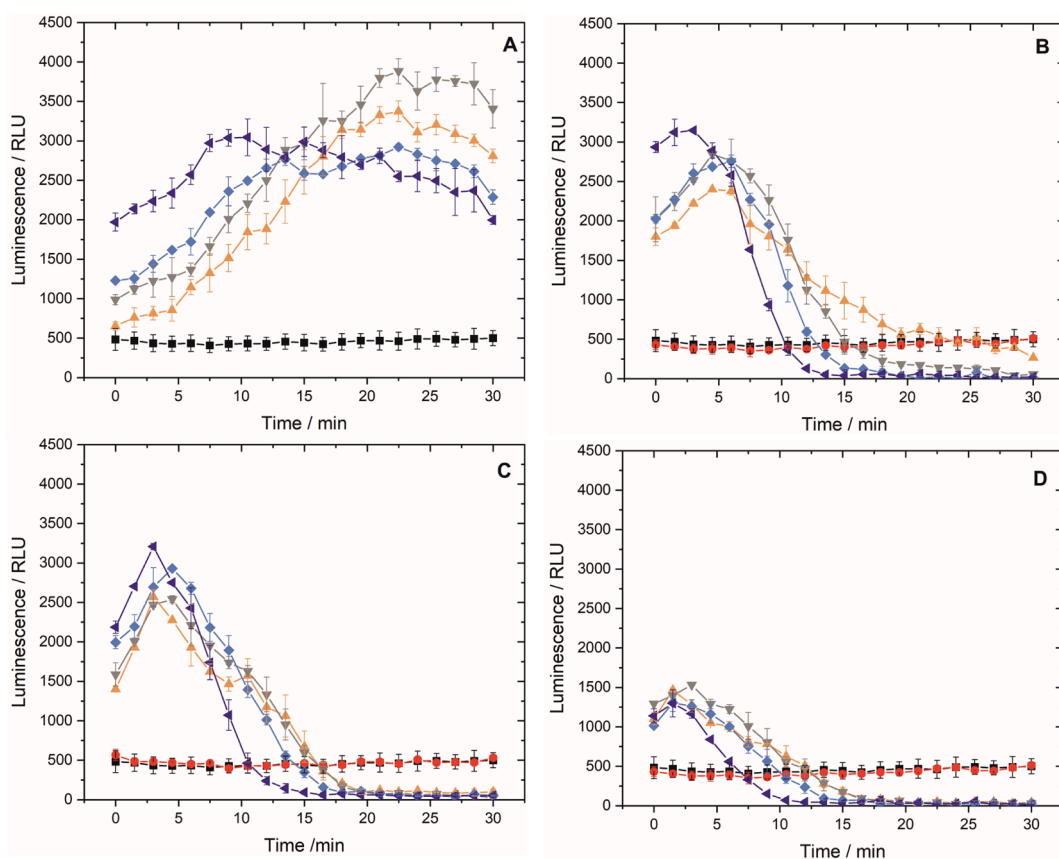


Fig. 2. The effects of μsPEF electroporation on the bioluminescence of the cells, where A – electroporation only treatment; B – electroporation with 2 mM calcium; C – electroporation with 5 mM calcium; D – electroporation with 10 mM calcium; \blacksquare – CTRL – buffer without added calcium; \bullet – buffer with added CaCl_2 ; \blacktriangle – $1.3 \text{ kV/cm} \times 100 \mu\text{s} \times 1$; \blacktriangledown – $1.3 \text{ kV/cm} \times 100 \mu\text{s} \times 2$; \blacklozenge – $1.3 \text{ kV/cm} \times 100 \mu\text{s} \times 4$; \blacktriangleleft – $1.3 \text{ kV/cm} \times 100 \mu\text{s} \times 8$.

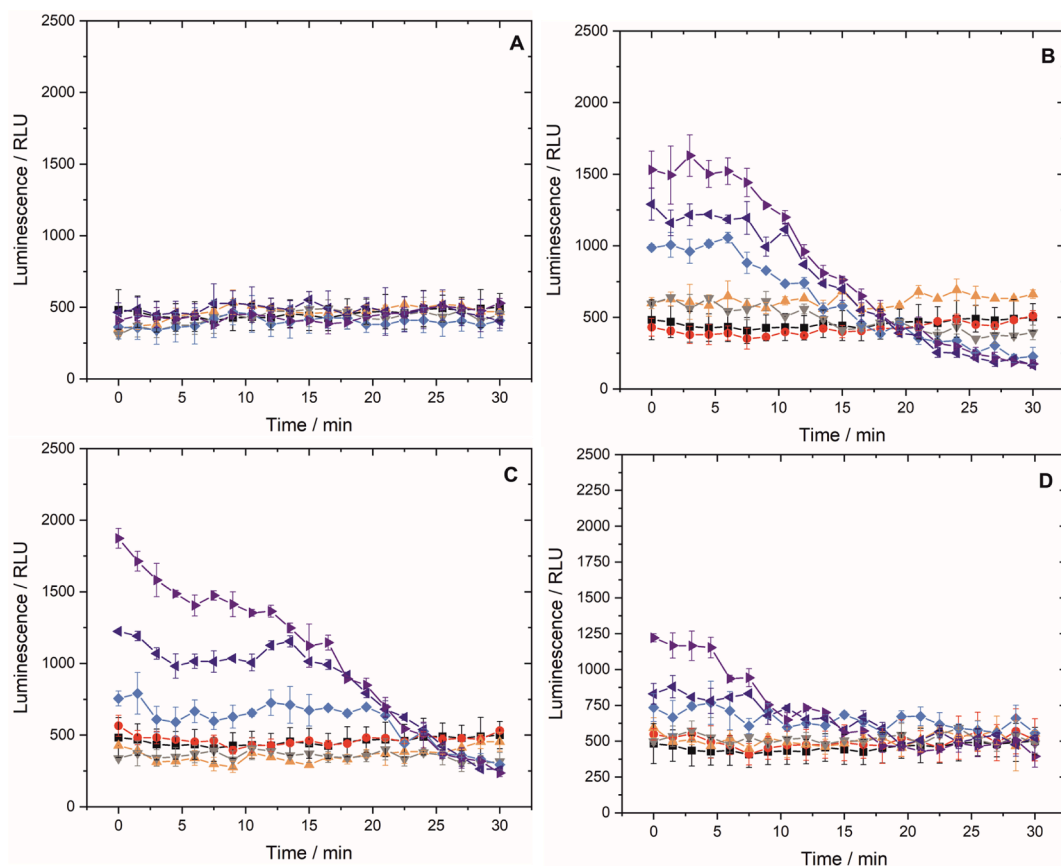


Fig. 3. The effects of kHz nsPEF electroporation (with and without added calcium) on the bioluminescence of the cells, where A – electroporation only treatment; B – electroporation with 2 mM calcium; C – electroporation with 5 mM calcium; D – electroporation with 10 mM calcium. —■— CTRL – buffer without added calcium; —●— buffer with added CaCl_2 ; —▲— 12.5 kV/cm \times 100 ns \times 5; —▼— 12.5 kV/cm \times 100 ns \times 10; —◆— 12.5 kV/cm \times 100 ns \times 25; —◀— 12.5 kV/cm \times 100 ns \times 50. —▶— 12.5 kV/cm \times 100 ns \times 100.

electroporation – the changes are beyond the detection limits. However, the addition of 2 mM Ca^{2+} improves the sensitivity of the assay, and a dose-dependent response can be observed too. For the 1 kHz and 1 MHz pulsing, the Pearson correlation coefficients between the assays are $R = 0.987$ and $R = 0.993$, respectively. In both cases, it is a strong positive correlation.

4. Discussion

We have presented a D-luciferin-based method of detection of cell electropermeabilization and compared the data with the uptake of a conventional nucleic acid dye YO-PRO-1. The cells have been permeabilized with μsPEF (100 μs) and nsPEF (100 ns) pulsed electric fields using 1.3 and 12.5 kV/cm electric field strengths, respectively. The number of pulses was varied in the range of 1–8 for μsPEF and in the range of 5–100 for the nsPEF protocols. Additionally, the effects of pulse repetition frequency (1 kHz/1 MHz) have been investigated. It was shown that the proposed bioluminescence-based methodology allows detection of electropermeabilization both in nanosecond and microsecond ranges. Also, kinetic measurements and multi-sample handling can be performed. We have used 1.5 min time steps to characterize the bioluminescent response and performed the measurement for 30 min. However, based on the requirements of the experiment, the time step can be reduced and the evaluation time increased. It was shown that the sensitivity of the proposed methodology to detect electropermeabilization is on par or slightly better than PI [19] for microsecond range electropermeabilization (using available infrastructure). In this work, the result was confirmed using YP (refer to Fig. 5). A dose-dependent response was observed for microsecond range pulses, with a high correlation between the assays (R

$= 0.929$).

In the case of nsPEF, detection of electropermeabilization might be a challenge, thus Ca, Ba ions, or in the worst case scenario YP is used [10]. In this study, we have used 100 ns pulses delivered at 1 kHz to trigger electropermeabilization, and no bioluminescent response was observed independently from the number of applied pulses. At the same time, YP showed permeabilized cells after 50 and 100 pulses. It implies that the methodology is less sensitive to detect electropermeabilization than YP, however, the situation changes with the addition of extracellular calcium. The statistically significant increase of bioluminescence was observed already after 25 pulses. A strong positive correlation between the YP and bioluminescent assays was observed both in 1 kHz and 1 MHz pulse regions. The effects of MHz pulsing were also covered in the study. As expected, the recently described phenomenon of increased permeabilization was triggered [24–27,29]. The sequences of the same intensity (12.5 kV/cm \times 100 ns) pulses delivered at MHz frequencies triggered higher electropermeabilization of the cells compared to 1 kHz protocols, which was confirmed by YP fluorescence and luciferin-luciferase assay. The sensitivity to detect electropermeabilization for 100 ns pulses was comparable between the assays with a high positive correlation of the results. It should be noted that we have used the $t = 0$ min data point to determine the capability to detect the electropermeabilization, which is not necessarily optimal. The reason is the different response dynamics (in terms of luminescent signal) between the different treatments. Choosing a specific time point when the luminescence is measured will affect the dynamic range and sensitivity and, thus, potentially can be optimized. However, we believe that for a proof-of-concept work choosing the $t = 0$ min was the best solution preventing bias. In the future the luciferin can be added to the cell medium prior to

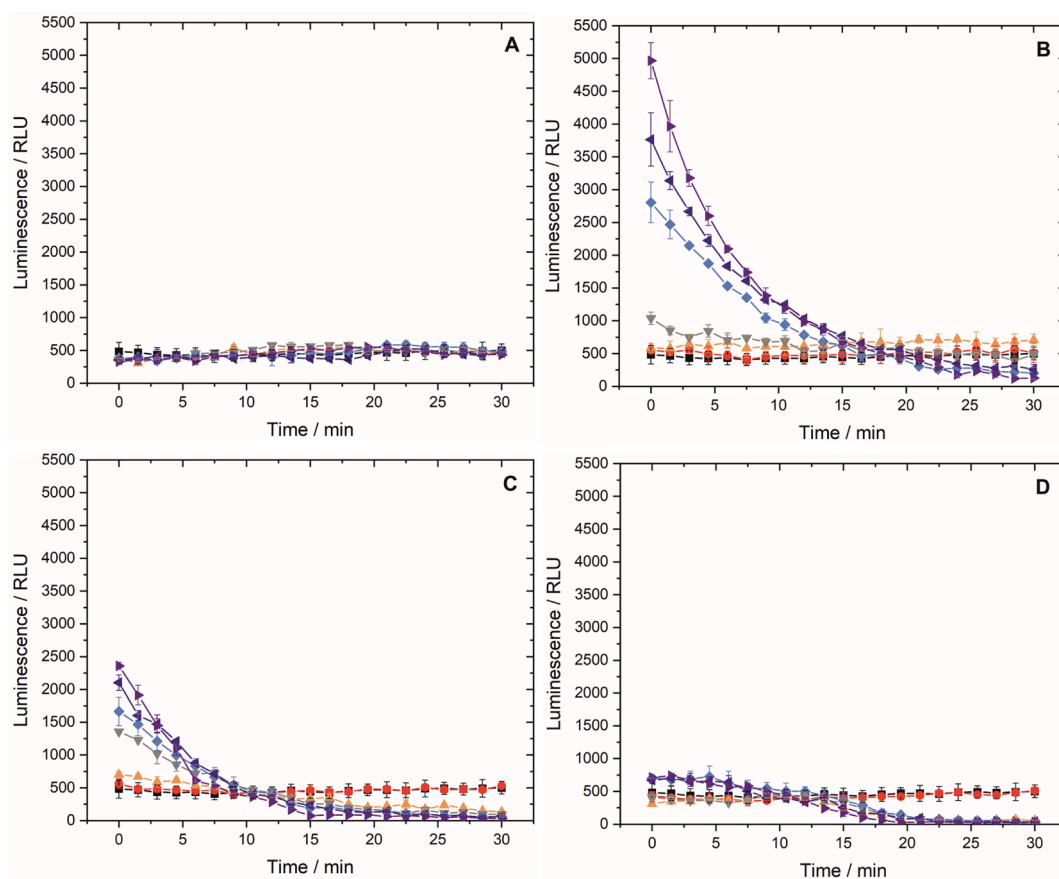


Fig. 4. The effects of MHz nsPEF electroporation (with and without added calcium) on the bioluminescence of the cells, where A – electroporation only treatment; B – electroporation with 2 mM calcium; C – electroporation with 5 mM calcium; D – electroporation with 10 mM calcium. —■— CTRL – buffer without added calcium; —●— buffer with added CaCl_2 ; —▲— 12.5 kV/cm \times 100 ns \times 5; —▼— 12.5 kV/cm \times 100 ns \times 10; —◆— 12.5 kV/cm \times 100 ns \times 25; —◀— 12.5 kV/cm \times 100 ns \times 50. —▶— 12.5 kV/cm \times 100 ns \times 100.

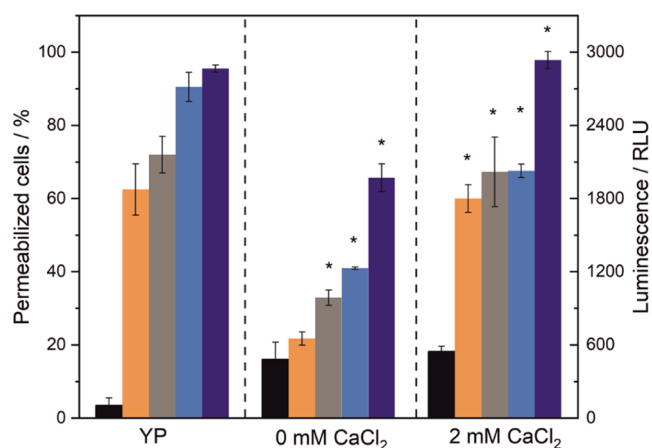


Fig. 5. Detection of μsPEF cell permeabilization using fluorescence (YP) and bioluminescence (d-luciferin oxidation), where ■ - untreated control; ■ - 1.3 kV/cm \times 100 μs \times 1; ■ - 1.3 kV/cm \times 100 μs \times 2; ■ - 1.3 kV/cm \times 100 μs \times 4; ■ - 1.3 kV/cm \times 100 μs \times 8. Asterisk (*) shows statistically significant ($p < 0.05$) difference versus control.

electroporation in a similar manner as YP is used. Such a methodological step may allow measuring the early kinetics of the signal, which are now missed since luciferin is added after electroporation. Therefore, methodology optimization works are a priority and are a matter of future works.

One of the most important results of the study is the scaling of the

luminescence signal with the addition of extracellular calcium. This phenomenon can be explained by the luciferin-luciferase assay signal scaling with ATP depletion [30,31]. With the increase of extracellular calcium concentrations, more calcium is delivered inside the cell by electroporation. Therefore, ATP is consumed by exchange pumps to stabilize (incl. pumps to extrude calcium from the cell) [32]. ATP depletion was reported for both nsPEF and μsPEF protocols [33–35], while calcium electroporation is known to trigger additional ATP depletion in the context of electroporation [22]. It partly explains why the peak values of luminescence (ATP depletion) during various treatments vary between the protocols (Table 1). It shows no controversy with available knowledge since cell injury between the protocols varies too (incl. membrane damage [36,37], mitochondrial damage [38,39], protein damage [40]). Also, the electrotransfer of calcium through such a damaged membrane depends on the electrophoretic component of the treatment, membrane porosity, and concentration gradient. In our work, a general tendency was observed that the luminescence signal increases if electroporation is triggered with the addition of calcium. However, the luminescence with 10 mM calcium treatment was several-fold lower compared to 2 mM treatments (refer to Table 1). Therefore, we speculate that the decrease of the luminescence during treatments with high concentration of calcium was associated with cytotoxicity of calcium. The 5 and 10 mM calcium concentrations are already beyond the thresholds, which are used in calcium electrochemotherapy *in vitro* [41,42]. Considering that only viable cells bioluminesce, the reduction of the RLU during high intensity treatments or with cytotoxic concentrations of calcium is only natural. This hypothesis should be checked in the future in order to support the applicability of the luciferin-luciferase methodology for indirect assessment of viability *in vitro*, however, it was

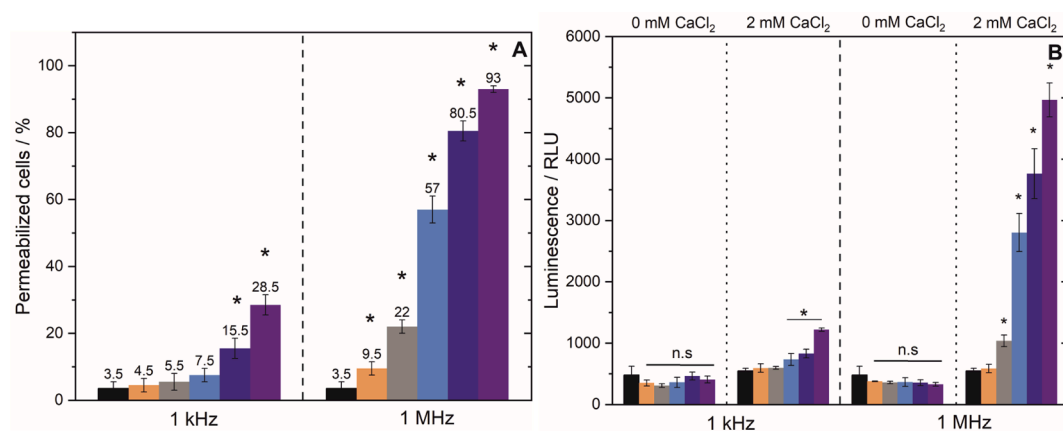


Fig. 6. Detection of nsPEF cell permeabilization using fluorescence (YP) and bioluminescence (d-luciferin oxidation), where ■ - untreated control; ■ - 12.5 kV/cm \times 100 ns \times 5; ■ - 12.5 kV/cm \times 100 ns \times 10; ■ - 12.5 kV/cm \times 100 ns \times 25; ■ - 12.5 kV/cm \times 100 ns \times 50. Asterisk (*) shows statistically significant ($p < 0.05$) difference versus control.

Table 1

Maximum luminescence after pulsed electric field treatment, asterisk (*) – statistically significant ($P < 0.05$) difference versus treatment without added calcium.

μ sPEF	RLU $\times 10^3$			
	No Ca	2 mM Ca	5 mM Ca	10 mM Ca
Protocol, 1 Hz				
1.3 kV/cm \times 100 μ s \times 1	3.4 \pm 0.1	2.4 \pm 0.01*	2.6 \pm 0.09*	1.5 \pm 0.02*
1.3 kV/cm \times 100 μ s \times 2	3.9 \pm 0.2	2.9 \pm 0.04*	2.5 \pm 0.05*	1.5 \pm 0.01*
1.3 kV/cm \times 100 μ s \times 4	2.9 \pm 0.04	2.8 \pm 0.08	2.9 \pm 0.03	1.3 \pm 0.08*
1.3 kV/cm \times 100 μ s \times 8	3 \pm 0.2	3.2 \pm 0.03	3.2 \pm 0.04	1.3 \pm 0.17*
nsPEF				
Protocol, 1 kHz				
12.5 kV/cm \times 100 ns \times 5	0.51 \pm 0.05	0.59 \pm 0.07	0.45 \pm 0.05	0.69 \pm 0.08*
12.5 kV/cm \times 100 ns \times 10	0.49 \pm 0.06	0.59 \pm 0.01	0.41 \pm 0.08	0.61 \pm 0.07
12.5 kV/cm \times 100 ns \times 25	0.47 \pm 0.09	0.77 \pm 0.15	0.76 \pm 0.05*	1.01 \pm 0.02*
12.5 kV/cm \times 100 ns \times 50	0.55 \pm 0.06	0.88 \pm 0.08*	1.22 \pm 0.01*	1.29 \pm 0.11*
12.5 kV/cm \times 100 ns \times 100	0.53 \pm 0.03	1.22 \pm 0.02*	1.87 \pm 0.07*	1.63 \pm 0.15*
nsPEF				
Protocol, 1 MHz				
12.5 kV/cm \times 100 ns \times 5	0.55 \pm 0.03	0.71 \pm 0.09*	0.7 \pm 0.05*	0.41 \pm 0.04
12.5 kV/cm \times 100 ns \times 10	0.58 \pm 0.03	1.04 \pm 0.1*	1.35 \pm 0.03*	0.46 \pm 0.04
12.5 kV/cm \times 100 ns \times 25	0.59 \pm 0.06	2.8 \pm 0.3*	1.67 \pm 0.22*	0.72 \pm 0.16
12.5 kV/cm \times 100 ns \times 50	0.53 \pm 0.02	3.76 \pm 0.41*	2.1 \pm 0.12*	0.7 \pm 0.03*
12.5 kV/cm \times 100 ns \times 100	0.55 \pm 0.01	4.97 \pm 0.28*	2.36 \pm 0.05*	0.74 \pm 0.02*

already confirmed for bacteria [43].

Additionally, our study did not focus on the effects of extracellular calcium on the membrane itself. Calcium is involved in membrane repair, pore stabilization, and resealing, so it might have an impact on the permeabilization results [44–46]. However, considering very positive correlations with YP methodology (which was performed without

calcium), the influence should be minor in the context of our study. Also, similar limitations apply to the conventional Ca^{2+} methodologies involving fluorophores.

5. Conclusions

It is concluded that the sensitivity of the luciferin-luciferase methodology to detect the electroporation is on par with YP uptake methodology when extracellular calcium is added. The delivery of nsPEF using MHz pulse repetition frequencies can improve the efficacy of electroporation several-fold compared to the equivalent low-frequency protocols. It was shown that the luciferin-luciferase methodology could be further applied for quantitative analysis of electroporation process *in vitro* (a dose-dependent response was acquired, with $R > 0.9$). However, further research is required to optimize the protocol and extend the dynamic range. Due to possibility to perform kinetic measurements, potentially, the luciferin-luciferase methodology could be used as a supporting tool in biophysical studies of electroporation, providing quantitative information on ATP, which is one of the main DAMPs (damage-associated molecular pattern molecules).

Declaration of Competing Interest

The authors declare that they have no known competing financial interests or personal relationships that could have appeared to influence the work reported in this paper.

Acknowledgements

We are grateful to the research professor Andrei Pakhomov from Old Dominion University for valuable comments, discussion, and advisory assistance with the preparation of this paper. The research was funded by the Research Council of Lithuania grant Nr. S-MIP-19-22 (PI: I. Girkontaite). The research was also partly funded by Polish National Science Centre grant Nr. 2016/22/E/NZ5/00671 (PI: J. Kulbacka) The funders had no role in study design, data collection and analysis, decision to publish, or preparation of the manuscript. The authors declare no conflict of interest.

References

- [1] A.G. Pakhomov, D. Miklavcic, M.S. Markov, Adv. Electroporation Techniq. Biol. Med. (2010), <https://doi.org/10.1201/ebk1439819067>.
- [2] E. Harris, J.J. Elmer, Optimization of electroporation and other non-viral gene delivery strategies for T cells, Biotechnol. Prog. 37 (1) (2021), <https://doi.org/10.1002/btpr.3066>.

- [3] O. Michel, J. Kulbacka, J. Saczko, J. Mączysińska, P. Błasiak, J. Rossowska, A. Rzechonek, Electroporation with cisplatin against metastatic pancreatic cancer: in vitro study on human primary cell culture, *Biomed. Res. Int.* 2018 (2018) 1–12, <https://doi.org/10.1155/2018/7364539>.
- [4] V.M. Ringel-Scalia, N. Beitel-White, M.F. Lorenzo, R.M. Brock, K.E. Huie, S. Coutermarsh-Ott, K. Eden, D.K. McDaniel, S.S. Verbridge, J.H. Rossmeisl, K. J. Oestreich, R.V. Davalos, I.C. Allen, High-frequency irreversible electroporation is an effective tumor ablation strategy that induces immunologic cell death and promotes systemic anti-tumor immunity, *EBioMedicine*. 44 (2019) 112–125, <https://doi.org/10.1016/j.ebiom.2019.05.036>.
- [5] V.J. Ferreira, A.J. Arnal, P. Royo, T. García-Armingol, A.M. López-Sabirón, G. Ferreira, Energy and resource efficiency of electroporation-assisted extraction as an emerging technology towards a sustainable bio-economy in the agri-food sector, *J. Clean. Prod.* 233 (2019) 1123–1132, <https://doi.org/10.1016/j.jclepro.2019.06.030>.
- [6] W. Sitzmann, E. Vorobiev, N. Lebovka, Applications of electricity and specifically pulsed electric fields in food processing: Historical backgrounds, *Innov. Food Sci. Emerg. Technol.* 37 (2016) 302–311, <https://doi.org/10.1016/j.ifset.2016.09.021>.
- [7] P. Bodénès, S. Bensalem, O. Français, D. Pareau, B. Le Pioufle, F. Lopes, Inducing reversible or irreversible pores in *Chlamydomonas reinhardtii* with electroporation: Impact of treatment parameters, *Algal Res.* 37 (2019) 124–132, <https://doi.org/10.1016/j.algal.2018.11.016>.
- [8] T. Polajžer, J. Dermol-Cerne, M. Reberšek, R. O'Connor, D. Miklavčič, Cancellation effect is present in high-frequency reversible and irreversible electroporation, *Bioelectrochemistry* 132 (2020) 107442, <https://doi.org/10.1016/j.bioelechem.2019.107442>.
- [9] T. Batista Napotnik, D. Miklavčič, In vitro electroporation detection methods – An overview, *Bioelectrochemistry* 120 (2018) 166–182, <https://doi.org/10.1016/j.bioelechem.2017.12.005>.
- [10] W. Bo, M. Silkunas, U. Mangalanathan, V. Novickij, M. Casciola, I. Semenov, S. Xiao, O.N. Pakhomova, A.G. Pakhomov, Probing nanoelectroporation and resealing of the cell membrane by the entry of Ca²⁺ and Ba²⁺ Ions, *Int. J. Mol. Sci.* 21 (9) (2020) 3386, <https://doi.org/10.3390/ijms21093386>.
- [11] H. Hanna, A. Denzi, M. Liberti, F.M. André, L.M. Mir, Electroporation of Inner and Outer Cell Membranes with Microsecond Pulsed Electric Fields: Quantitative Study with Calcium Ions, *Sci. Rep.* 7 (1) (2017), <https://doi.org/10.1038/s41598-017-12960-w>.
- [12] S.J. Bae, D.J. Im, Evaluation of cell viability and delivery efficiency in electroporation system according to the concentrations of propidium iodide and yo-pro-1, *Korean Chem. Eng. Res.* (2019), <https://doi.org/10.9713/keer.2019.57.6.898>.
- [13] A.G. Pakhomov, S. Grigoryev, I. Semenov, M. Casciola, C. Jiang, S. Xiao, The second phase of bipolar, nanosecond-range electric pulses determines the electroporation efficiency, *Bioelectrochemistry* 122 (2018) 123–133, <https://doi.org/10.1016/j.bioelechem.2018.03.014>.
- [14] Y. Ye, X. Luan, L. Zhang, W. Zhao, J. Cheng, M. Li, Y. Zhao, C. Huang, Single-cell electroporation with real-time impedance assessment using a constriction microchannel, *Micromachines*. 11 (9) (2020) 856, <https://doi.org/10.3390/mi11090856>.
- [15] A.M. Bowman, O.M. Nesin, O.N. Pakhomova, A.G. Pakhomov, Analysis of plasma membrane integrity by fluorescent detection of TI(+) uptake, *J. Membr. Biol.* 236 (1) (2010) 15–26, <https://doi.org/10.1007/s00232-010-9269-y>.
- [16] E.C. Gianulis, C. Labib, G. Saulis, V. Novickij, O.N. Pakhomova, A.G. Pakhomov, Selective susceptibility to nanosecond pulsed electric field (nsPEF) across different human cell types, *Cell. Mol. Life Sci.* 74 (9) (2017) 1741–1754, <https://doi.org/10.1007/s00118-016-2434-4>.
- [17] I. Semenov, S. Xiao, O.N. Pakhomova, A.G. Pakhomov, Recruitment of the intracellular Ca²⁺ by ultrashort electric stimuli: the impact of pulse duration, *Cell Calcium* 54 (3) (2013) 145–150, <https://doi.org/10.1016/j.ceca.2013.05.008>.
- [18] L. Towhidi, T. Kotnik, G. Pucihar, S.M.P. Firoozabadi, H. Mozdarani, D. Miklavčič, Variability of the minimal transmembrane voltage resulting in detectable membrane electroporation, *Electromagn. Biol. Med.* 27 (4) (2008) 372–385, <https://doi.org/10.1080/15368370802394644>.
- [19] V. Novickij, A. Zinkevičienė, V. Malysko, J. Novickij, J. Kulbacka, N. Rembalkowska, I. Girkontaitė, Bioluminescence as a sensitive electroporation indicator in sub-microsecond and microsecond range of electrical pulses, *J. Photochem. Photobiol. B Biol.* 213 (2020) 112066, <https://doi.org/10.1016/j.jphotobiol.2020.112066>.
- [20] M. Endo, Calcium ion as a second messenger with special reference to excitation-contraction coupling, *J. Pharmacol. Sci.* 100 (5) (2006) 519–524, <https://doi.org/10.1254/jphs.CPJ06004X>.
- [21] R.J. Kaufman, J.D. Malhotra, Calcium trafficking integrates endoplasmic reticulum function with mitochondrial bioenergetics, *Biochim. Biophys. Acta - Mol. Cell Res.* 1843 (10) (2014) 2233–2239, <https://doi.org/10.1016/j.bbamcr.2014.03.022>.
- [22] E.L. Hansen, E.B. Sozer, S. Romeo, S.K. Frandsen, P.T. Vernier, J. Gehl, B. Rubinsky, Correction: Dose-Dependent ATP Depletion and Cancer Cell Death following Calcium Electroporation, Relative Effect of Calcium Concentration and Electric Field Strength, *PLoS One* 10 (4) (2015) e0122973, <https://doi.org/10.1371/journal.pone.0122973>, <https://doi.org/10.1371/journal.pone.0122973.g00110.1371/journal.pone.0122973.g00210.1371/journal.pone.0122973.g00310.1371/journal.pone.0122973.g00410.1371/journal.pone.0122973.g00510.1371/journal.pone.0122973.t001>.
- [23] M.P. Rols, J. Teissié, Electroporation of mammalian cells. Quantitative analysis of the phenomenon, *Biophys. J.* 58 (5) (1990) 1089–1098, [https://doi.org/10.1016/S0006-3495\(90\)82451-6](https://doi.org/10.1016/S0006-3495(90)82451-6).
- [24] Z.A. Steelman, G.P. Tolstykh, H.T. Beier, B.L. Ibey, Cellular response to high pulse repetition rate nanosecond pulses varies with fluorescent marker identity, *Biochem. Biophys. Res. Commun.* 478 (3) (2016) 1261–1267, <https://doi.org/10.1016/j.bbrc.2016.08.107>.
- [25] I. Semenov, M. Casciola, B.L. Ibey, S. Xiao, A.G. Pakhomov, Electroporation of cells by closely spaced paired nanosecond-range pulses, *Bioelectrochemistry* 121 (2018) 135–141, <https://doi.org/10.1016/j.bioelechem.2018.01.013>.
- [26] V. Novickij, P. Ruzgys, A. Grainys, S. Šatkauskas, High frequency electroporation efficiency is under control of membrane capacitive charging and voltage potential relaxation, *Bioelectrochemistry* 119 (2018) 92–97, <https://doi.org/10.1016/j.bioelechem.2017.09.006>.
- [27] A. Murauskas, G. Staigvila, I. Girkontaitė, A. Zinkevičienė, P. Ruzgys, S. Šatkauskas, J. Novickij, V. Novickij, Predicting electrotransfer in ultra-high frequency sub-microsecond square wave electric fields, *Electromagn. Biol. Med.* 39 (1) (2020) 1–8, <https://doi.org/10.1080/15368378.2019.1710529>.
- [28] V. Novickij, A. Grainys, P. Butkus, S. Tolvaišienė, J. Švedienė, A. Paskevicius, J. Novickij, High-frequency submicrosecond electroporation, *Biotechnol. Biotechnol. Equip.* 30 (3) (2016) 607–613, <https://doi.org/10.1080/13102818.2016.1150792>.
- [29] A.G. Pakhomov, S. Xiao, V. Novickij, M. Casciola, I. Semenov, U. Mangalanathan, V. Kim, C. Zemlin, E. Sozer, C. Muratori, O.N. Pakhomova, Excitation and electroporation by MHz bursts of nanosecond stimuli, *Biochem. Biophys. Res. Commun.* 518 (4) (2019) 759–764, <https://doi.org/10.1016/j.bbrc.2019.08.133>.
- [30] A. Lundin, Optimization of the firefly luciferase reaction for analytical purposes, *Adv. Biochem. Eng. Biotechnol.* (2014), https://doi.org/10.1007/978-3-662-43619-6_2.
- [31] M.V. Zamaraeva, R.Z. Sabirov, E. Maeno, Y. Ando-Akatsuka, S.V. Bessonova, Y. Okada, Cells die with increased cytosolic ATP during apoptosis: A bioluminescence study with intracellular luciferase, *Cell Death Differ.* 12 (11) (2005) 1390–1397, <https://doi.org/10.1038/sj.cdd.4401661>.
- [32] S.T. Cooper, P.L. McNeil, Membrane Repair: Mechanisms and Pathophysiology, *Physiol. Rev.* 95 (4) (2015) 1205–1240.
- [33] R. Nuccitelli, A. McDaniel, S. Anand, J. Cha, Z. Mallon, J.C. Berridge, D. Uecker, Nano-Pulse Stimulation is a physical modality that can trigger immunogenic tumor cell death, *J. Immunother. Cancer* 5 (2017) 32, <https://doi.org/10.1186/s40425-017-0234-5>.
- [34] A. Rossi, O.N. Pakhomova, P.A. Mollica, M. Casciola, U. Mangalanathan, A. G. Pakhomov, C. Muratori, Nanosecond pulsed electric fields induce endoplasmic reticulum stress accompanied by immunogenic cell death in murine models of lymphoma and colorectal cancer, *Cancers (Basel)* 11 (12) (2019) 2034, <https://doi.org/10.3390/cancers11122034>.
- [35] T. Polajžer, T. Jarm, D. Miklavčič, Analysis of damage-associated molecular pattern molecules due to electroporation of cells in vitro, *Radiol. Oncol.* 54 (3) (2020) 317–328, <https://doi.org/10.2478/raon-2020-0047>.
- [36] O.N. Pakhomova, B.W. Gregory, I. Semenov, A.G. Pakhomov, M.R. Scarfi, Two Modes of Cell Death Caused by Exposure to Nanosecond Pulsed Electric Field, *PLoS One* 8 (7) (2013) e70278, <https://doi.org/10.1371/journal.pone.0070278>, <https://doi.org/10.1371/journal.pone.0070278.g00110.1371/journal.pone.0070278.g00210.1371/journal.pone.0070278.g00310.1371/journal.pone.0070278.g00410.1371/journal.pone.0070278.g00510.1371/journal.pone.0070278.g00610.1371/journal.pone.0070278.g00710.1371/journal.pone.0070278.g00810.1371/journal.pone.0070278.g009>.
- [37] S.J. Beebe, J. White, P.F. Blackmore, Y. Deng, K. Somers, K.H. Schoenbach, Diverse Effects of Nanosecond Pulsed Electric Fields on Cells and Tissues, *DNA Cell Biol.* 22 (12) (2003) 785–796, <https://doi.org/10.1089/104454903322624993>.
- [38] S.J. Beebe, Y.-J. Chen, N.M. Sain, K.H. Schoenbach, S. Xiao, A. Guerrero-Hernandez, Transient Features in Nanosecond Pulsed Electric Fields Differentially Modulate Mitochondria and Viability, *PLoS ONE* 7 (12) (2012) e51349, <https://doi.org/10.1371/journal.pone.0051349>, <https://doi.org/10.1371/journal.pone.0051349.g00110.1371/journal.pone.0051349.g00210.1371/journal.pone.0051349.g00310.1371/journal.pone.0051349.g00410.1371/journal.pone.0051349.g00510.1371/journal.pone.0051349.g006>.
- [39] W.E. Ford, W. Ren, P.F. Blackmore, K.H. Schoenbach, S.J. Beebe, Nanosecond pulsed electric fields stimulate apoptosis without release of pro-apoptotic factors from mitochondria in B16f10 melanoma, *Arch. Biochem. Biophys.* 497 (1–2) (2010) 82–89, <https://doi.org/10.1016/j.abb.2010.03.008>.
- [40] S.J. Beebe, Considering effects of nanosecond pulsed electric fields on proteins, *Bioelectrochemistry* 103 (2015) 52–59, <https://doi.org/10.1016/j.bioelechem.2014.08.014>.
- [41] J. Kulbacka, N. Rembalkowska, A. Szewczyk, H. Moreira, A. Szyjka, I. Girkontaitė, K.P. Grela, V. Novickij, The Impact of Extracellular Ca²⁺ and Nanosecond Electric Pulses on Sensitive and Drug-Resistant Human Breast and Colon Cancer Cells, *Cancers* 2021, Vol. 13, Page 3216. 13 (2021) 3216, <https://doi.org/10.3390/cancers13133216>.
- [42] S.K. Frandsen, L. Gibot, M. Madi, J. Gehl, M.P. Rols, Calcium electroporation: Evidence for differential effects in normal and malignant cell lines, evaluated in a 3D spheroid model, *PLoS One*. (2015). <https://doi.org/10.1371/journal.pone.0144028>.
- [43] V. Novickij, A. Zinkevičienė, R. Stanevičienė, R. Gruskiene, E. Servienė, I. Vepšaitė-Monstavičė, T. Krivorotova, E. Lastauskiene, J. Sereikaitė, I. Girkontaitė, J. Novickij, Inactivation of *Escherichia coli* Using Nanosecond Electric Fields and Nisin Nanoparticles: A Kinetics Study, *Front. Microbiol.* 9 (2018) 3006, <https://doi.org/10.3389/fmicb.2018.03006>.

- [44] F. Ciobanu, M. Golzio, E. Kovacs, J. Teissié, Control by Low Levels of Calcium of Mammalian Cell Membrane Electroporation, *J. Membr. Biol.* 251 (2) (2018) 221–228, <https://doi.org/10.1007/s00232-017-9981-y>.
- [45] S. Bhattacharya, M. Silkunas, E. Gudvangen, U. Mangalanathan, O.N. Pakhomova, A.G. Pakhomov, Ca²⁺ dependence and kinetics of cell membrane repair after electroporation, *Biochim. Biophys. Acta - Biomembr.* 1864 (2) (2022) 183823, <https://doi.org/10.1016/j.bbamem.2021.183823>.
- [46] D. Navickaitė, P. Ruzgys, M. Maciulevičius, G. Dijk, R.P. O'Connor, S. Šatkauskas, Ca²⁺ roles in electroporation-induced changes of cancer cell physiology: From membrane repair to cell death, *Bioelectrochemistry* 142 (2021) 107927, <https://doi.org/10.1016/j.bioelechem.2021.107927>.